JOURNAL OF SYNCHROTRON RADIATION

ISSN 1600-5775

Characterization of an X-ray mirror mechanical bender for the European XFEL

Maurizio Vannoni,* Idoia Freijo Martín and Harald Sinn

European XFEL, Hamburg, Germany. *Correspondence e-mail: maurizio.vannoni@xfel.eu

Received 23 December 2015
Accepted 7 April 2016

Edited by G. E. Ice, Oak Ridge National Laboratory, USA

Keywords: bendable mirror; X-ray optics; active optics; metrology.

One of the classical devices used to tune a mirror on an X-ray optical setup is a mechanical bender. This is often designed in such a way that the mirror is held with clamps on both ends; a motor is then used to put a torque on the clamps, inducing a cylindrical shape of the mirror surface. A mechanical bender with this design was recently characterized, to bend a 950 mm-long mirror up to a radius of curvature of 10 km. The characterization was performed using a large-aperture Fizeau interferometer with an angled incidence setup. Some particular and critical effects were investigated, such as calibration, hysteresis, twisting and long-term stability.

1. Introduction

To be effective in the majority of experiments, the X-ray beam produced by synchrotron and free-electron laser (FEL) sources needs to be focused in a certain position, usually where the sample has been placed. In some optical setups, an intermediate focus is also created in the beam transport, between the undulator source and the ultimate focusing system. This is often the case for very long optical setups, to avoid the natural expanding of the beam. In most cases, the focusing of the beam is achieved using curved optical elements, such as Kirkpatrick–Baez (KB) mirrors, and the exact positioning of the focus can be tuned either by changing the radius of curvature of the mirrors or by rotating them to a different incidence angle. The latter method also requires a direction correction to align the beam again, and it is limited in range. For this reason, directly changing the shape of the mirror using a bender is usually preferred, thus moving the focus position accordingly. Another application of bendable or deformable mirrors is to compensate for non-uniform heating of the mirror reflecting surface because of a thermal gradient, or to compensate polishing errors.

One method of building a bendable X-ray system is to mechanically clamp the mirror on the edges and then introduce a symmetric torque on both sides (see, for example, Ferme, 1997). According to classical beam theory (Timoshenko, 1953; Ugural & Fenster, 1995), the torque creates a perfectly cylindrical shape. In some designs, it is even possible to apply a different torque on the two ends, causing an elliptical shape if the thickness of the mirror is chosen accordingly (Howells *et al.*, 2000; McKinney *et al.*, 2009). The interaction between the mechanical system and the mirror is very critical. Mechanical tolerances are not precise enough to prevent the clamp supports from applying significant preload forces during the installation of the mirror in the bender. These forces affect the mirror surface, as we report in §3.1. To achieve the correct shape, a time-consuming fine-tuning is often necessary.

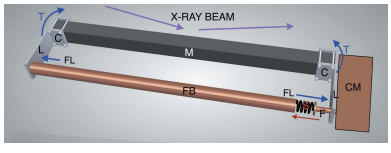

Table 1
Fizeau measuring system specifications.

Manufacturer, distributor	Zygo, AMETEK Germany GmbH
Model	Dynafiz plus 12-inches expander
Measuring principle	Phase-shift interferometry
Aperture	304.8 mm
Source	Stabilized He–Ne laser, wavelength λ = 632.8 nm
Repeatability	<0.25 nm (2σ)
Resolution	$\lambda/12000$ (high-resolution mode, double pass)
Image size	1200 × 1200 pixels
Digitization	10 bits
Flats quality (calibrated)	12 nm and 18 nm (P–V)
Flats material	Fused silica

Another limitation is that the entire system is supported by flexures or springs, causing the mirror to vibrate or drift due to mechanical stresses and temperature changes. On the other hand, having flexures to support the clamps means that the bending of the mirror remains in the purely elastic regime; for this reason, the design should be very smooth and reproducible, with no 'jumps' from one radius of curvature to another because of non-reproducible friction effects.

Because of the required fine-tuning, it is in effect mandatory to check the mirror with a proper measuring instrument before the final installation. In our case, we used a large-aperture Fizeau system (Table 1).

The main reason for using a Fizeau interferometer is that this instrument is relatively fast and effective: it can deliver a two-dimensional map of the test surface in a few seconds. Even when performing averaging, which can take a few minutes, this is still sufficient to make numerous adjustments in a short time. We used the Fizeau instrument to properly install the mirror inside the mechanical bender, to help with the initial fine-tuning of the system, and later to calibrate its bending capabilities in an absolute way. Additional investigations regarding hysteresis and long-term stability were also carried out.

2. Description of the mechanical bender system

The measured mechanical bender system was built by FMB Oxford (Oxford, UK). It is a classical U-bender with the levers attached to the clamps where the mirror is supported without any additional gravity compensation. The bending effect is achieved by pushing on the two levers with an actuator, thereby introducing a torque on the mirror clamps. In our case, a stepper motor drives a cam mechanism, thereby pushing a mechanical follower, which compresses a spring against a long bar (named 'force bar'). The force bar pushes one of the levers, introducing a torque on one mirror end through the clamp. An identical force is applied to the follower, which transmits the force to the cam; the motor and the cam are rigidly connected to the second lever, so in the end the effect is to also produce a torque on the second end of the mirror (Fig. 1). The levers are connected to the supporting plate (not shown in the figure) with mechanical flexures, designed such that the fixed points during the bending of the mirror are close to the middle longitudinal line. The flexures move together with the mirror during the bending, so the behaviour is very close to being fully elastic. The only point that experiences some dynamical friction effect is in the cam mechanism.

The system is designed for inducing a small correction of the shape of the mirror, which has to be maintained close to flatness, so the range of bending is relatively small. The step motor has an additional gear box to increase sensitivity. To estimate the bender performances, we consider a simplified mathematical model. In a U-bender, a symmetrical moment of forces M is applied to a mirror with momentum of inertia I:

$$R = EI/M, \tag{1}$$

where R is the radius of curvature of the mirror due to the bending and E is Young's modulus. In our case, the mirror has a squared section of side w; therefore, the momentum of inertia is $I = w^4/12$. The moment $M = Fh$ is introduced using a force F applied on the levers of length h. The force $F = kx$ is created by the spring with spring constant k, compressed by an amount x. The final relationship is thus

$$R = \frac{E(w^4/12)}{kxh}. \tag{2}$$

The corresponding sag s is then

$$s = \frac{L^2}{8R} = \frac{3}{2}\frac{L^2 kxh}{Ew^4}. \tag{3}$$

A description of all of the parameters and their nominal values is given in Table 2.

In this report, instead of describing the variation of the radius of curvature, we plot the total sag of the mirror as defined as in equation (3). The parameters listed in Table 2 are fixed for a given bender, defining the total range and sensitivity. The only exception is the spring, which is designed to be replaceable. We evaluate the impact of these parameters on

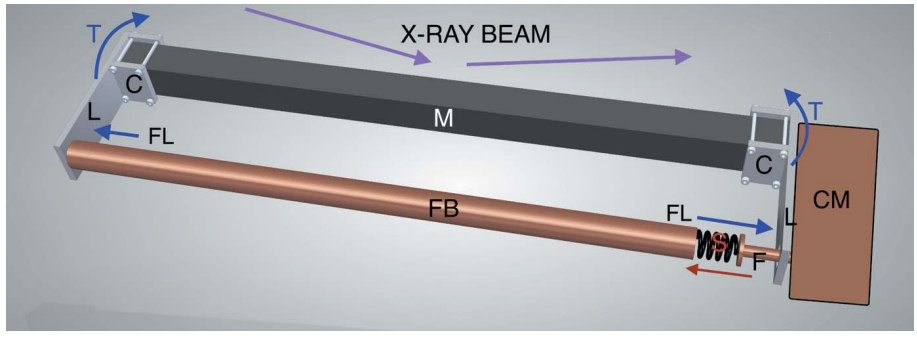

Figure 1
Schematic of the mechanical bender: the mirror (M) is supported by the clamps (C) attached to levers (L). The cam mechanism (CM, here not detailed for property-rights reasons) pushes the follower (F), compressing the spring (S) against the force bar (FB). Because of the compression of the spring, reaction forces are applied to the levers (FL), creating a torque (T) on the mirror ends.

Table 2
Mechanical bender model parameters.

Description	Symbol	Nominal value	Unit
Radius of curvature	R		m
Sag	s		m
Momentum of inertia	I		m
Spring constant	k	8.89×10^3	N m^{-1}
(stiffer spring)		(39.37×10^3)	N m^{-1}
Length of levers	h		m
Young's modulus of silicon	E	130×10^9	Pa
Mirror thickness/width	w	52×10^{-3}	m
Mirror length	L	0.95	m

the tested system in §4. The exact value of each parameter is not known with enough accuracy to provide an absolute calibration of the bender, so we needed to measure it using a previously calibrated instrument, in this case a Fizeau interferometer.

3. Characterization of the system using a large-aperture Fizeau interferometer

To obtain an independent measurement of the mirror surface, including the bending induced by the mechanical system, we used a large-aperture Fizeau interferometer, similarly to our testing of a piezo-bender in previous work (Vannoni *et al.*, 2016). The system was placed inside a long optical cavity created using two 12-inch diameter flats (Fig. 2).

The corresponding interference pattern was created and analysed. The calibration of the Fizeau instrument is linked to the absolute shape of the two flats, which are absolutely calibrated by the vendor with an uncertainty better than 20 nm peak-to-valley (P–V). The measurements described in this paper were carried out under standard environment conditions and not in vacuum.

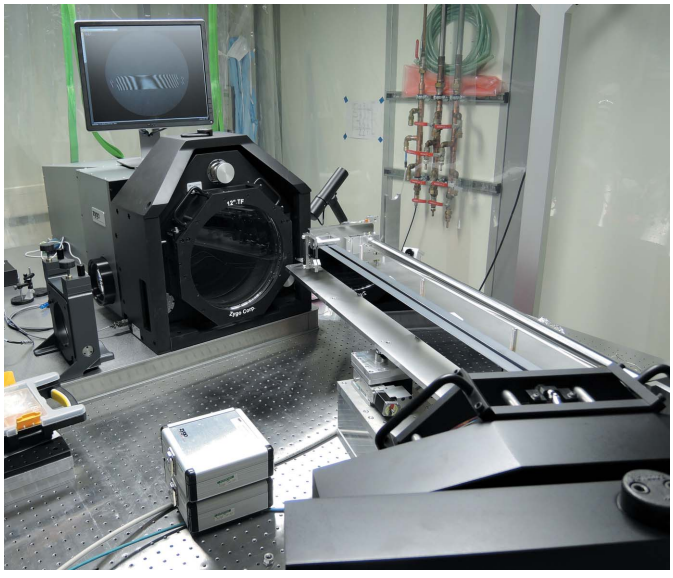

Figure 2
Photograph of the mechanical bendable mirror placed between two auxiliary optical flats, creating an optical cavity in an angled incidence setup. The screen above the beam expander shows an image of the interference fringes.

3.1. First installation of the mirror in the bender

When installing the mirror in the bender, first the clamps need to be placed on both sides. The clamps are designed as an open cage: each end of the mirror is placed inside the clamp and fixed, and the screws are tightened with dynamometric tools (Fig. 1). Contact is made directly between the metal and the silicon, with the mirror held by friction. Then the mirror is mounted on the bender using two kinematic mounts, one for each clamp.

One of the characteristics of this particular design is that the spring can only be compressed, so the mirror can be bent only in the direction of being more concave. Even in the unbent position, it is very difficult to start from a perfectly flat mirror because of the spring preload, which always applies some initial curvature. This problem can be partially solved by putting some initial preload on the clamps, but this method is not very reproducible and it should be improved in a future release of the bender. Because of this problem, the initial state of the mirror can change slightly for every new installation of the system or after replacement of the spring. In our particular application, only very small adjustments around the best flat are needed, so it would be better to start from a slightly convex shape at the zero position to improve the range of adjustment around flatness. This is probably a special case compared with the main use of these benders in general focusing systems.

Another characteristic of the design is that the mirror can twist. The positioning of the two kinematic mounts supporting the mirror cannot be perfectly symmetrical. This difference creates a rotational torque along the length of the mirror, and the effect is enhanced by the relatively small aspect ratio of the mirror, $w/L = 0.055$ in our case. The mechanics provide a compensation mechanism for such a twist, and the result can be checked using the interferometer to reach the best possible situation. To obtain a quantitative evaluation of the twist, we analysed the measured surface, taking many longitudinal sections along the mirror and calculating the variation of the profile tilt angle for different distances from the centre. An example of such an optimization process is presented in Fig. 3.

3.2. Characterization of the bending capabilities

The mirror is bent by the movement of the motor actuator, and the corresponding surface shape is measured using the Fizeau interferometer. The movement is limited by two end switches, from 0 to 165 (arbitrary units) with one step motor corresponding to an amount of 9.78×10^{-3}. In our calibration procedure, we activated the motor to create bending, waited a certain amount of time to reach a stable situation, and then measured the corresponding centre profile along the mirror length. The behaviour of the bender is highly elastic and has a fast response, so the waiting time between reaching a position and performing the measurement was set to only 5 min, as a precautionary amount of time to enable vibrations of the table and residual stresses on the bender mechanics to fade out; it can probably be even smaller in real operation. In Fig. 4, we

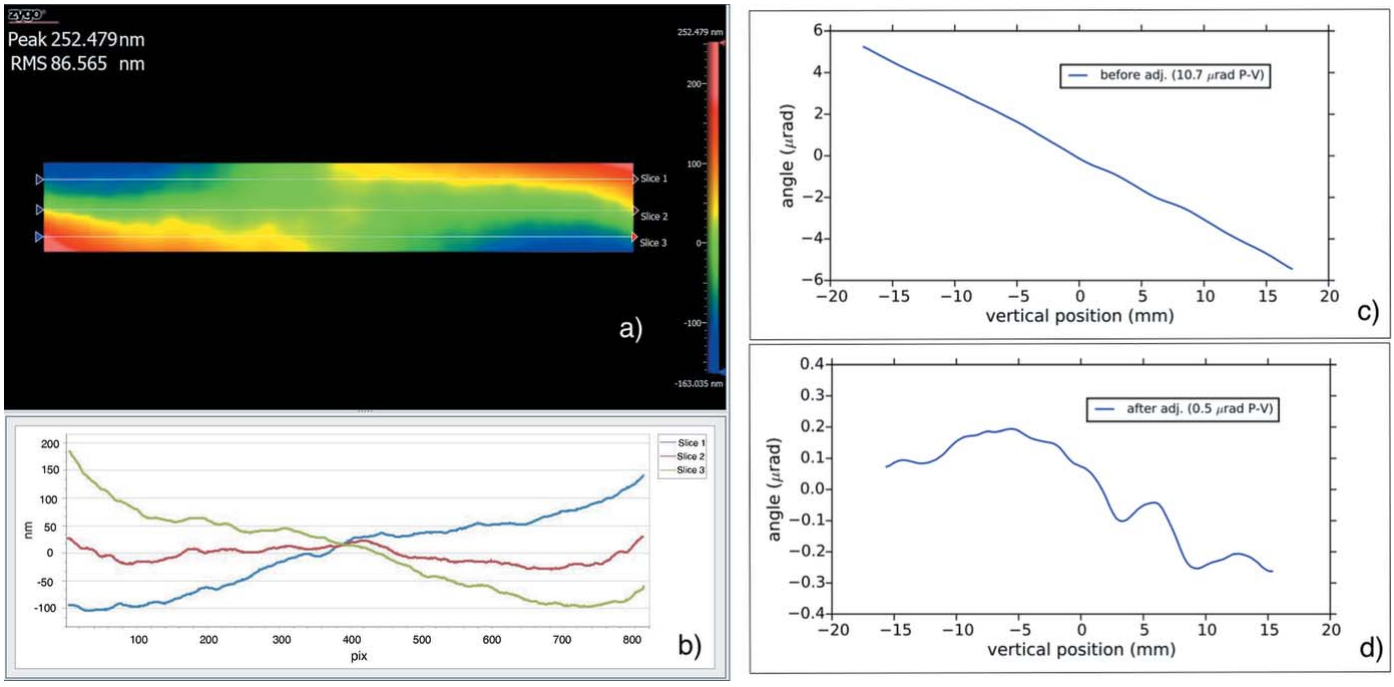

Figure 3
Evaluation of the mirror twist in a given situation. Two-dimensional map measurement (*a*) with three longitudinal profiles corresponding to different positions (*b*). Situation before (*c*) and after (*d*) the twist adjustment.

report the result in terms of centre profiles obtained for some bending positions.

We calculated the corresponding radius of curvature of each position (Fig. 5) by taking the best-fitting parabolas of the measured profiles. This is a Taylor series approximation of the theoretical cylindrical curve, and the difference between them is negligible for long radii of curvature, as in this case.

The profiles reported in Fig. 4 are very close to parabolas. We can give a quantitative measurement of that, removing the best parabola from every profile. The remaining part (Fig. 6) is intrinsically related to the mirror residual polishing of the mirror: it is therefore the same for every profile with some repeatability because of the instrument and the environment, that can be accounted as an average r.m.s. of 1.6 nm. This value was determined by extracting the average profile from Fig. 6, calculating the r.m.s. of each profile and calculating the mean r.m.s. value. The P–V height is one order of magnitude higher.

The mirror used for the testing is a classically polished mirror: it has the same shape and material as the future European XFEL mirrors, but its surface quality is lower compared with what is specified for the European XFEL beam transport system. Nevertheless, its quality is sufficient for our testing purposes.

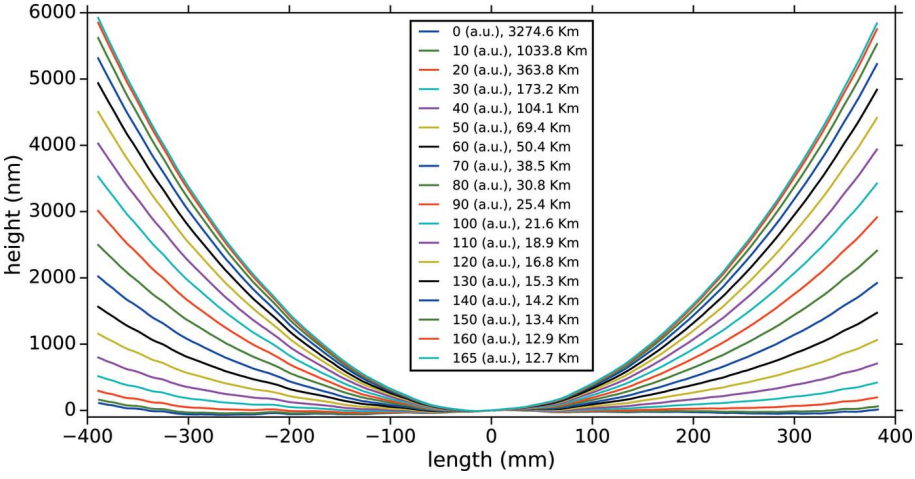

Figure 4
Measured centre profiles obtained for several bending positions.

3.3. Hysteresis effect

Most of the structure of the bender is based on flexures to minimize any friction forces creating 'stick and slip' effects. One of the few parts of the design where friction cannot be avoided is inside the cam mechanism. We found that friction can also occur in other parts of the system, *e.g.* in the spring enclosure or in the mechanical part surrounding the follower. This can be improved with a better installation of the mechanics. To account for these effects and fine-tune the system, we repeated the bending measurement reported in Fig. 5 several times, moving the motor back and forth and checking whether any differences occurred for

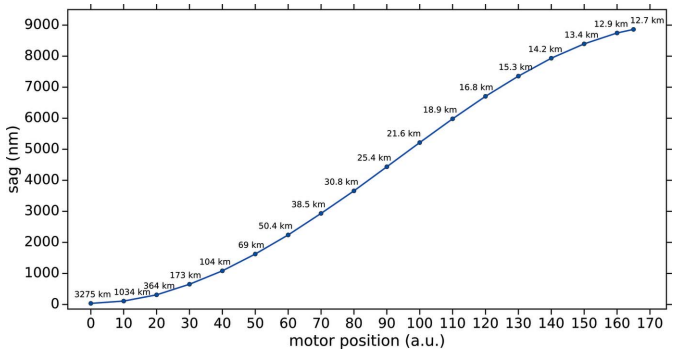

Figure 5
Best-fitting radius of curvature *versus* position of the motor.

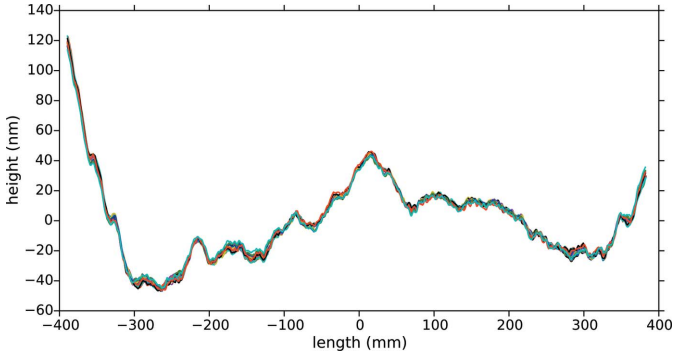

Figure 6
Measured centre profiles, with the best-fitting parabola removed.

the different directions. In this way, the installation can be optimized. To demonstrate the difference, we report a case with some hysteresis (Fig. 7*a*) and another case in which a better fine-tuning of the mechanics was achieved (Fig. 7*b*).

In the best case, reported in Fig. 7(*b*), some differences between the individual scans remain, which are better visible when the average calibration curve is subtracted (Fig. 8).

Part of the differences is probably related to variations of the temperature inside the laboratory, which is stable up to 0.1°C in the short term but not stable enough to avoid small drifts of the mirror curvature, as we will see in §5. The environmental repeatability also influences the result, but only in the range 10–20 nm P–V in the measured sag.

4. Calibration of the bender with a stiffer spring and comparison with the theoretical model

One interesting feature of the presented system is the possibility of changing the spring on the force bar, thereby changing the range and the sensitivity of the bending accordingly. When using a stiffer spring with spring constant k = 39.37 N mm^{-1}, we obtained the result shown in Fig. 9.

As can be seen from the negative sag at the zero position of the motor, this time we adjusted the initial preload of the mirror so as to generate a slightly convex shape. We can compare the calibration curves with our theoretical model in equation (3) using a fitting curve,

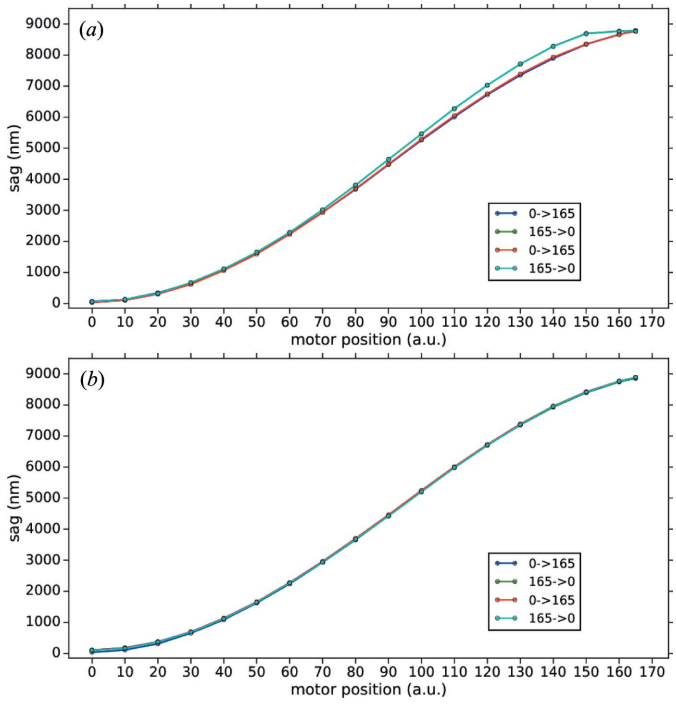

Figure 7
Measured hysteresis curve in a case with some friction inside the system (*a*) and after better tuning of the mechanics (*b*).

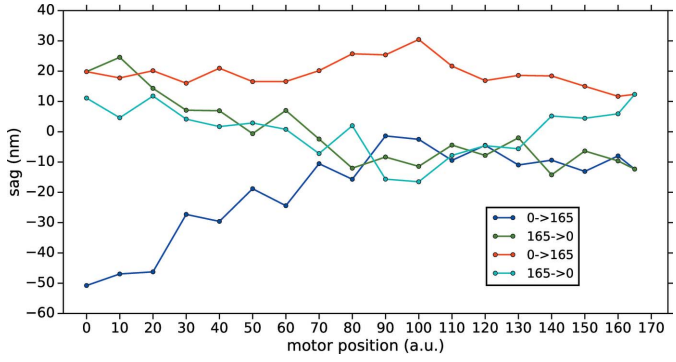

Figure 8
Residual hysteresis in the best situation, taking the profiles and subtracting the average calibration curve.

$$s = P_1\left[1 - \cos(\theta + P_2)\right] + P_3, \tag{4}$$

where P_1 is the amplitude, P_2 is the initial phase and P_3 is the initial bending due to the preload. Performing the calculation for the two springs, we found the results shown in Table 3. The relatively large difference between the nominal and fitted values is considered normal, due to the high uncertainty on the nominal value of the parameters and especially on the spring constant k.

5. Dependence of the radius of curvature on temperature and long-term stability

The dependence of the bending on temperature is intrinsic to the design of the mechanical bender. We could expect an important effect from the force bar, due to its length and the

Table 3
Best-fitting results for the calibration curves.

	Parameter		
	P_1 (m)	P_2 (a.u.)	P_3 (m)
Softer spring (nominal)	5.06×10^{-6}	0	0
Softer spring (fitting)	4.47×10^{-6}	−1.6	0.123×10^{-6}
Stiffer spring (nominal)	22.4×10^{-6}	0	0
Stiffer spring (fitting)	32.8×10^{-6}	−3.4	-2.75×10^{-6}

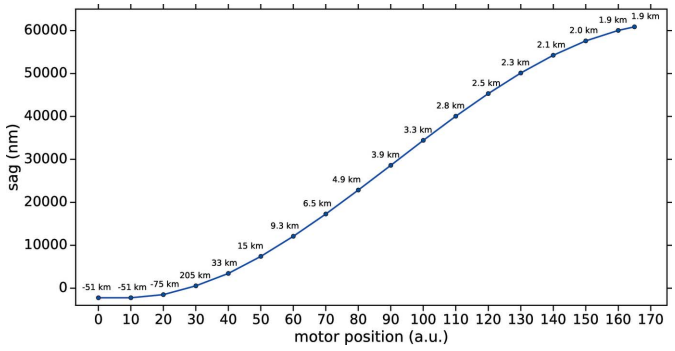

Figure 9
Calibration curve using a stiffer spring with $k = 39.37$ N mm^{-1} (nominal).

related thermal expansion. However, this effect is negligible in practice, as we can easily demonstrate. If the force bar is made of aluminium, with a linear expansion coefficient of $\alpha = 22.6 \times 10^{-6}$ m (m K)$^{-1}$, a temperature change of 0.1°C will induce an expansion of 2.1 µm, corresponding to a change in sag of 4.5 nm in the most sensitive position of the cam. In reality, we measured a variation approximately one order of magnitude higher (Fig. 10).

To perform the measurement, we connected a four-wire Pt100 sensor to the bender, measuring its temperature with a Keithley 2700 multimeter. We turned on the room ventilation to allow a limited exchange of air with the external hall, thereby producing a slow cooling of the ambient temperature. The temperature of the bender was measured over 24 h while the Fizeau interferometer carried out automatic measurements every half an hour. From the average angle of the two curves, we estimated a change in sag of 53 nm for a temperature variation of 0.1°C. We think that this effect comes from the entire mechanical holder rather than just from the force bar. We verified that the effect was not induced by the Fizeau interferometer itself by repeating the measurements with the simple cavity made by the two flats without the bender in between. The stability of the Fizeau instrument was in the range 10–20 nm P–V in the measured sag for a temperature change of more than 1°C, that is, much less than the effect seen with the bender in the setup.

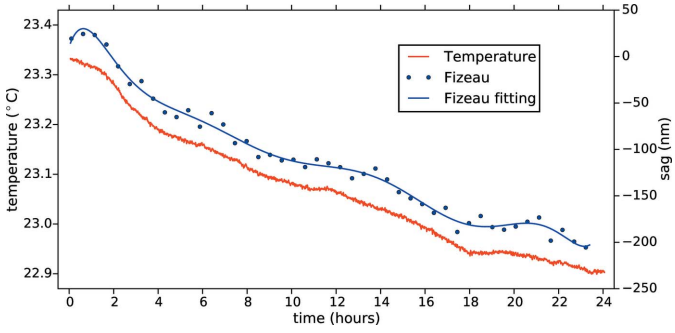

Figure 10
Profile variations over a relatively long time period.

6. Discussion of results and final conclusions

We have presented an extensive investigation of a mechanical U-bender for X-ray optics, providing a precise characterization of the bender and its fine-tuning. The mirror was adjusted for twisting and initial load, enabling a quantitative measurement of the residual shape. The mirror was then calibrated within its designed range, allowing us to check how close the system is to a simple mechanical model and finding the best-fitting parameters to describe its behaviour. Using the hysteresis curve measurement, it was possible to verify whether the installation was done in the right way and whether residual friction effects were still present. The system was always very responsive, fast to stabilize, and the behaviour can be considered in the elastic regime.

The main problem that we detected is the high sensitivity of the system to temperature variations, as we pointed out in §5. This could result in two important effects. The first effect would be a shift of the performed calibration, reported in Figs. 5 and 9, in case the mirror is installed in an environment with a different temperature. We could forecast the shift and correct it using the measurement carried out in Fig. 10. The second effect would appear during use, with small differences in the temperature of the device resulting in a long-term drift of the radius of curvature. Again, the basic idea for correcting this effect would be to measure the temperature to correct the bending or to introduce another kind of feedback to control the drift. Another problem we found is caused by the preload, which has no fine-tuning, resulting in a slightly different situation every time the mirror is installed again. A calibration with the Fizeau interferometer would help to check the situation, but a better tuning would make the process faster and easier.

Acknowledgements

We would like to thank FMB Oxford for providing us with useful information about the details of the mechanical bender.

References

Ferme, J.-J. (1997). *Proc. SPIE*, **3152**, 103.
Howells, M. R., Cambie, D., Duarte, R. M., Irick, S., MacDowell, A. A., Padmore, H. A., Renner, T. R., Rah, S. & Sandler, R. (2000). *Opt. Eng.* **39**, 2748–2762.
McKinney, W. R., Kirschman, J. L., MacDowell, A. A., Warwick, T. & Yashchuk, V. V. (2009). *Opt. Eng.* **48**, 083601.
Timoshenko, S. (1953). *History of Strength of Materials.* New York: McGraw-Hill.
Ugural, A. C. & Fenster, S. K. (1995). *Advanced Strength and Applied Elasticity.* Englewood Cliffs: Prentice Hall.
Vannoni, M., Freijo Martín, I., Siewert, F., Signorato, R., Yang, F. & Sinn, H. (2016). *J. Synchrotron Rad.* **23**, 169–175.